ChemSusChem

Full Papers
doi.org/10.1002/cssc.202101932

Chemistry Europe
European Chemical Societies Publishing

www.chemsuschem.org

Comparative Performance of PETase as a Function of Reaction Conditions, Substrate Properties, and Product Accumulation

Erika Erickson,[a, b] Thomas J. Shakespeare,[b, c] Felicia Bratti,[a, b] Bonnie L. Buss,[a, b] Rosie Graham,[b, c] McKenzie A. Hawkins,[a, b] Gerhard König,[c] William E. Michener,[a, b] Joel Miscall,[a, b] Kelsey J. Ramirez,[a, b] Nicholas A. Rorrer,[a, b] Michael Zahn,[c] Andrew R. Pickford,[b, c] John E. McGeehan,*[b, c] and Gregg T. Beckham*[a, b]

There is keen interest to develop new technologies to recycle the plastic poly(ethylene terephthalate) (PET). To this end, the use of PET-hydrolyzing enzymes has shown promise for PET deconstruction to its monomers, terephthalate (TPA) and ethylene glycol (EG). Here, the *Ideonella sakaiensis* PETase wild-type enzyme was compared to a previously reported improved variant (W159H/S238F). The thermostability of each enzyme was compared and a 1.45 Å resolution structure of the mutant was described, highlighting changes in the substrate binding cleft compared to the wild-type enzyme. Subsequently, the performance of the wild-type and variant enzyme was compared as a function of temperature, substrate morphology, and reaction mixture composition. These studies showed that reaction temperature had the strongest influence on performance between the two enzymes. It was also shown that both enzymes achieved higher levels of PET conversion for substrates with moderate crystallinity relative to amorphous substrates. Finally, the impact of product accumulation on reaction progress was assessed for the hydrolysis of both PET and bis(2-hydroxyethyl) terephthalate (BHET). Each enzyme displayed different inhibition profiles to mono(2-hydroxyethyl) terephthalate (MHET) and TPA, while both were sensitive to inhibition by EG. Overall, this study highlights the importance of reaction conditions, substrate selection, and product accumulation for catalytic performance of PET-hydrolyzing enzymes, which have implications for enzyme screening in the development of enzyme-based polyester recycling.

Introduction

Enzymatic depolymerization of poly(ethylene terephthalate) (PET) is a promising approach for recycling of this abundant polyester.[1] Multiple PET hydrolases have been identified and characterized,[2] including the PETase enzyme from *Ideonella sakaiensis*.[3] *Is*PETase, together with a second enzyme, MHETase, forms a two-enzyme system for the conversion of PET to its monomers, terephthalic acid (TPA) and ethylene glycol (EG).[4] Using *Is*PETase as a model system, numerous engineering studies have been reported that present modified enzymes with improved thermal stability and catalytic activity relative to the wild-type enzyme.[5] Of relevance to this work, a mutant variant of *Is*PETase (W159H/S238F) was previously reported,[6] where two amino acid substitutions modify the enzyme's active site to more closely match that of a cutinase from *Thermobifida fusca*, TfCut2.[7]

Here, we present an assessment of enzymatic performance for the wild-type *Is*PETase[3,5a,c,8] (hereafter, WT) and a double mutant variant (W159H/S238F) (hereafter, DM) to understand the implications of altering the active site of this mesophilic PET hydrolase to more closely resemble that of a thermophilic cutinase. Performance is compared across factors likely to impact hydrolysis rate and conversion extent, including reaction temperature, reaction mixture composition, agitation during hydrolysis, enzyme loading, substrate loading, and product accumulation. These studies highlight the impacts of reaction conditions on catalytic performance, where reaction rates, substrate specificity, and inhibition can be significantly different even for two closely related enzymes. This has important implications for the development of PET-active biocatalysts, especially when considering enzyme screening strategies for process-relevant PET hydrolases.[9]

[a] *Dr. E. Erickson, F. Bratti, Dr. B. L. Buss, M. A. Hawkins, W. E. Michener, J. Miscall, K. J. Ramirez, Dr. N. A. Rorrer, Dr. G. T. Beckham*
Renewable Resources and Enabling Sciences Center
National Renewable Energy Laboratory
Golden, CO 80401 (United States)
E-mail: Gregg.Beckham@nrel.gov

[b] *Dr. E. Erickson, T. J. Shakespeare, F. Bratti, Dr. B. L. Buss, R. Graham, M. A. Hawkins, W. E. Michener, J. Miscall, K. J. Ramirez, Dr. N. A. Rorrer, Prof. A. R. Pickford, Prof. J. E. McGeehan, Dr. G. T. Beckham*
BOTTLE Consortium
Golden, CO 80401 (United States)

[c] *T. J. Shakespeare, R. Graham, Dr. G. König, Dr. M. Zahn, Prof. A. R. Pickford, Prof. J. E. McGeehan*
Centre for Enzyme Innovation
School of Biological Sciences
Institute of Biological and Biomedical Sciences
University of Portsmouth
Portsmouth PO1 2DY (United Kingdom)
E-mail: John.McGeehan@port.ac.uk

Supporting information for this article is available on the WWW under https://doi.org/10.1002/cssc.202101932

This publication is part of a Special Collection highlighting "The Latest Research from our Board Members". Please visit the Special Collection at chemsuschem.org/collections.

Results

Structural and biophysical comparison of the W159H/S238F variant of *Is*PETase reveals conformational and stability changes compared to the WT

To compare structural differences between the WT and DM, a high-resolution X-ray crystal structure of the DM was solved with diffraction data extending to a resolution of 1.45 Å (PDB ID: 7OSB) (Figure 1, Figure S1, Table S1). The two amino acid substitutions (W159H/S238F) (Figure 1) in the DM induce narrowing of the active site cleft (Figure 1B) compared to the WT enzyme (PDB ID: 6EQE)[6] (Figure 1E), and otherwise result in minimal conformational changes to the structure (Figure S2).

Despite the small change in overall structure, these point mutations have a marked effect on the thermal stability of the DM enzyme relative to the WT (Figure 1D, Figure S3). The apparent T_m of the WT is 46.76 ± 0.04 °C, measured by differential scanning calorimetry (DSC), while the apparent T_m of the DM is 56.49 ± 0.22 °C (Figure 1D). In comparing the thermodynamic stability (resistance to thermal unfolding) of each enzyme as a function of temperature, the WT and DM enzymes have comparable stability at 30 °C (Figure S3A). As the temperature increases, the relative stability of the DM compared to the WT increases, reaching a maximum relative difference in stability at 47 °C (Figure S3B). At 47 °C, the WT has a 19 fold increased propensity for thermal denaturation compared to the DM at the same temperature.

Substrates used in this study include amorphous and crystalline PET

The primary PET substrates utilized for all studies include an amorphous film (2.0 ± 1.6% crystallinity), a biaxially oriented film (30.7 ± 5.5% crystallinity), and a crystalline powder (37.7 ± 2.6% crystallinity), all sourced from Goodfellow, unless noted otherwise. Detailed characterization of each substrate used in these studies was performed (Table S2).[9a]

DMSO in the reaction mixture promotes conversion of amorphous PET film

PET hydrolysis reaction parameters reported in the literature vary widely. In some studies, dimethyl sulfoxide (DMSO) is included in the reaction[3,4,6,11] to promote solubility of liberated monomers. In other studies, DMSO is not included,[2a,b,7,12] leading us to study the influence of DMSO on PET conversion. Likewise, some studies have included agitation of the reaction to facilitate mass transfer and promote association between the enzyme and the substrate.[12,13] To understand if either inclusion of DMSO in the reaction mixture or agitation of the reaction during hydrolysis appreciably influence the extent of PET conversion, we compared reactions over 96 h using both the WT and DM incubated at 30 and 40 °C (Figure 2, Figure S4). All reactions were performed using 1 mg g^{-1} enzyme loading and 2.9% by mass (29 g L^{-1}) substrate loading of an amorphous PET

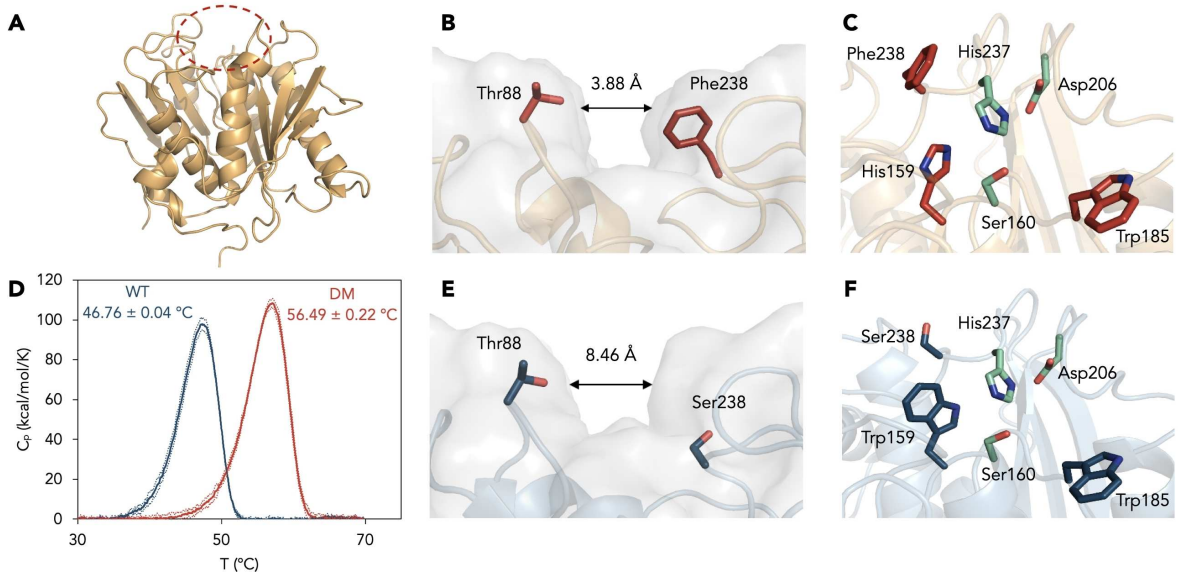

Figure 1. Structural comparison of the DM and WT *Is*PETase enzymes. (A) Ribbon representation of the structure of the DM *Is*PETase at 1.45 Å resolution (PDB ID: 7OSB). The active site cleft at the top is indicated with a dashed red circle. (B) View along the active site cleft of the DM enzyme. The width of the cleft measures 3.88 Å between the oxygen of Thr88 and the nearest carbon of Phe238, accounting for the Van Der Waal's radius of each atom. (C) Close-up of active site residues of the DM enzyme. The catalytic triad residues (Ser160, Asp206, His237) are highlighted in green. The mutated residues (His159, Phe238, orange) are shown alongside Trp185 (orange), which is predicted to be critical in providing the PET polymer access to the active site.[10] (D) Calorimetric enthalpy curves showing the molar specific heat capacity (C_p) of the enzyme in solution as a function of temperature for the WT and DM enzymes. The apparent T_m of each enzyme is indicated. Solid lines represent the average, and the faint dotted lines indicate the standard deviation range measured over three biological replicates. (E) The active site cleft of WT *Is*PETase (blue) is wider than the DM enzyme with a width of 8.46 Å between the oxygen of Thr88 and the nearest carbon of Ser238. (F) Comparative view of the WT *Is*PETase active site with the catalytic triad residues (green). Residues Ser238 and Trp159 (blue) are shown alongside Trp185 (blue). Information about the structure is provided in Table S1.

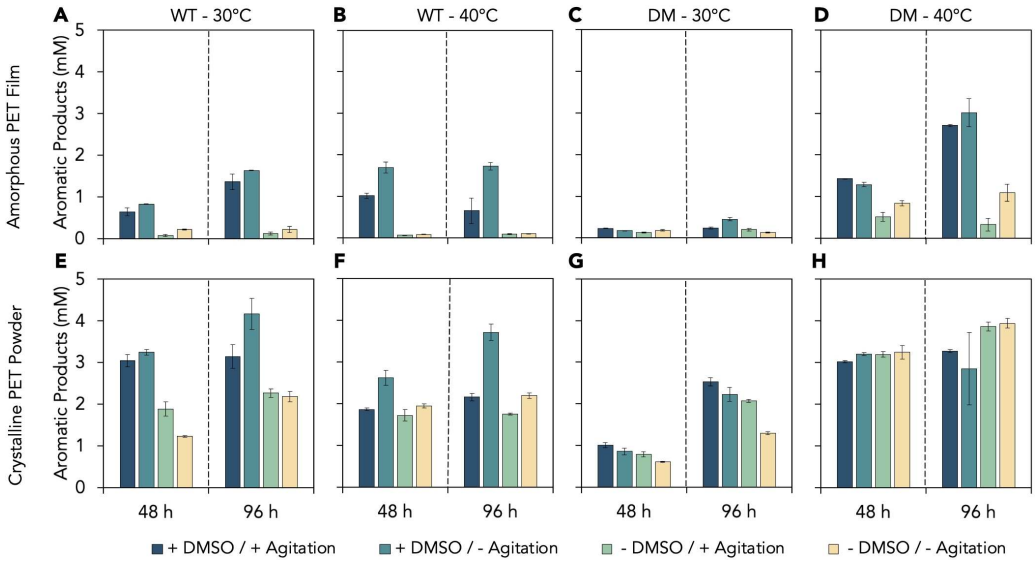

Figure 2. Contribution of agitation and DMSO to product release. Enzymatic conversion of PET reported as the sum of aromatic products released from (A–D) an amorphous PET film substrate, and (E–H) a crystalline PET powder substrate at 48 and 96 h for the WT and DM. Graphs show a comparison of reactions with and without 10% DMSO in the reaction mixture, and with or agitation of the reaction, using an orbital shaker. All reactions were performed in duplicate and error bars represent the absolute error between replicates. Progress curves showing aromatic product release over 96 h are available for each dataset in Figure S4. Information about statistical analysis of these datasets is in Table S3. All reactions were performed in duplicate. The data for these plots are in Dataset S1.

film and a crystalline PET powder (Table S2). The reaction buffer for samples without DMSO (−DMSO) was 50 mM NaH_2PO_4, 100 mM NaCl, pH 7.5. The solvent inclusion condition (+DMSO) was performed using a buffer comprising 90% (*v*/*v*) 50 mM NaH_2PO_4, 100 mM NaCl, 10% (*v*/*v*) DMSO, pH 7.5. Agitation was performed using an incubated orbital shaker at 225 rpm.

In comparing product release between PET substrates, this study highlights the impact of substrate selection on conversion extent. For both enzymes in most reaction conditions, a 2–5 fold increase in total product release is measured for reactions containing crystalline powder compared to the same mass loading of an amorphous film (Figure 2). These results also highlight that the WT and the DM have different temperature-dependent activity profiles, where a change of 10 °C in the reaction temperature has a larger differential effect on catalytic performance for the DM at 48 and 96 h reaction times.

In general, product release was highest in the presence of DMSO, while agitation resulted in slightly less product release, on average. Reactions without DMSO tended to reach a lower PET conversion extent over 48 and 96 h, which is most apparent for reactions with amorphous PET. The DM enzyme on crystalline PET exhibits the least variation in PET conversion across all four conditions tested (Figure 2G,H). As the +DMSO/-Agitation condition generally resulted in the highest PET conversion, all subsequent reactions presented subsequently were performed using this reaction condition, unless noted otherwise.

Reaction progress and endpoint analysis reveal differential activity profiles for the WT and DM enzymes

Hydrolytic performance on PET was evaluated for the WT and DM at 30 and 40 °C to assess how the difference in apparent T_m might influence the rate and extent of PET conversion. The lower temperature is the isolation temperature of the host organism[3] and the typical reaction temperature reported for *Is*PETase activity. The higher temperature, which is below the apparent T_m of the WT, was selected to identify if increased temperature would result in faster conversion.

Conversion extent was evaluated by substrate mass loss and measurement of the aromatic monomers released [as the sum of bis(2-hydroxyethyl) terephthalate (BHET), mono(2-hydroxyethyl) terephthalate (MHET), and TPA]. The effect of reaction temperature was examined over 168 h using two enzyme loadings [0.2 mg enzyme g^{-1} PET (Figure S5, Table S4) and 1.0 mg enzyme g^{-1} PET (Figure 3, Table S5)], and a substrate loading of 2.9% by mass (29 g L^{-1}) of amorphous PET film. The resulting trend in reaction progress curves is similar for both enzymes at both enzyme loadings, where reactions incubated at 40 °C accumulate more aromatic product at early time points (<48 h) (Figure 3A). For the WT, at 40 °C product accumulation plateaus by 48 h, while at 30 °C the enzyme continues hydrolyzing amorphous PET film through the 168 h timepoint. The DM exhibits low relative activity at 30 °C, but at 40 °C remains active through 168 h and accumulates the highest total concentration of aromatic product monomer from 72 h onward.

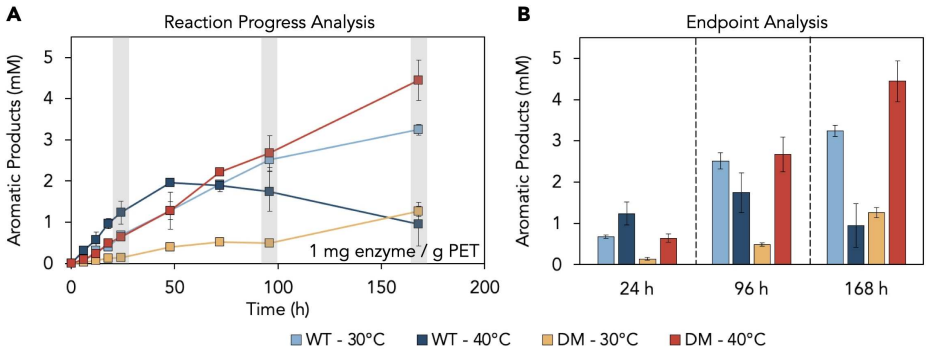

Figure 3. Reaction progress analysis and endpoint analysis comparing the WT and DM *Is*PETase enzymes across reaction temperatures. Sacrificial samples were generated for each timepoint. Each reaction contains 1 mg enzyme g^{-1} PET and 2.9% amorphous PET film by mass (29 g L^{-1}). Reactions were evaluated for 168 h to compare enzyme stability. (A) Progress curves show variation in total aromatic product release over time for each condition evaluated. (B) Three different endpoint analyses, at 24, 96, and 168 h provide three different performance comparisons between the WT and DM. There is no significant difference in product release between WT-30 °C and DM-40 °C reactions at both 24 and 96 h according to 2-way ANOVA multiple comparison. Additional statistical analysis information is in Table S6. Error bars represent the standard deviation of reactions performed in triplicate. Datasets for these plots are in Dataset S2.

Catalytic efficiency and substrate affinity are improved at 40 °C for both the WT and DM

In addition to conversion extent, we also evaluated initial rates of hydrolysis for the WT and DM using the conventional (convMM) and inverse (invMM) Michaelis-Menten (MM) kinetic models.[14] The convMM model examines reaction regimes in which the substrate is present in great excess of the biocatalyst, while the invMM model is a study with enzyme in excess of the substrate. Given the nature of the insoluble PET substrates hydrolyzed by these enzymes, achieving the conditions required for the convMM reactions is not trivial, and therefore we explored both kinetic models. Using the kinetic parameters derived from these models, we can compare the performance of each enzyme by comparing affinity between the enzyme and the substrate ($^{conv}K_m$, Equation S1 and $^{inv}K_m$, Equation S2) and maximal reaction velocity ($^{conv}V_{max}$, Equation S3 and $^{inv}V_{max}$, Equation S4).

Specifically, sacrificial samples were generated for each time point over a reaction time of 6–10 h (while initial reaction rates remain linear). Kinetic parameters were determined by fitting for both enzymes at 30 and 40 °C on two different PET substrates, amorphous PET film and a crystalline PET powder. Initial rate measurements were collected for the convMM dataset (Figure 4, Table 1) using 950 nM enzyme and varying the substrate loading over a range of 0–11.6% by mass (0–116 g L^{-1}) to identify a saturating substrate load, or when substrate is sufficiently in excess that all enzymes in the reaction are engaged. Initial rate measurements were also collected for the invMM dataset (Figure 5, Table 1) using a substrate loading of 2.9% by mass (29 g L^{-1}) and varying the enzyme loading over a range of 0–2 mg enzyme per g PET

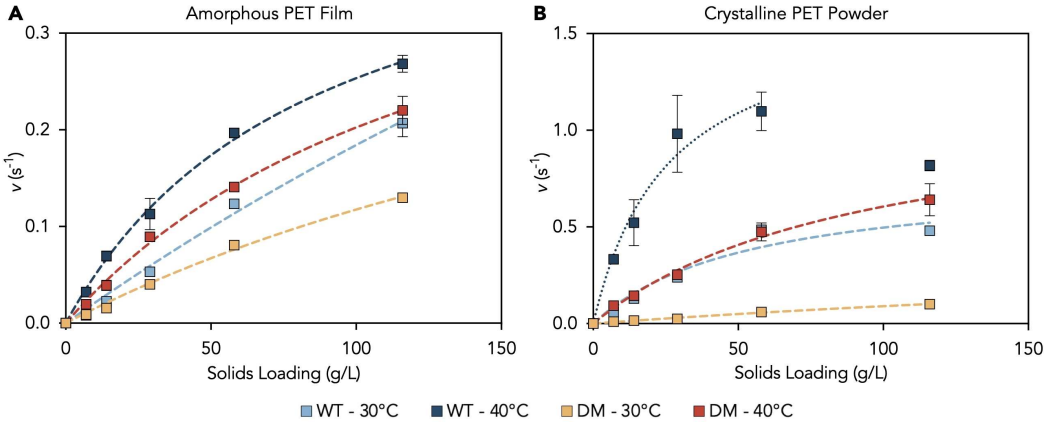

Figure 4. Conventional Michaelis-Menten plots at 30 and 40 °C. The plots show PET hydrolysis rates as a function of substrate loading [g L^{-1}]. Square symbols represent turnover rates determined from experimental data using 950 nM enzyme and 0–116 g L^{-1} substrate. The derived kinetic parameters are in Table 1. Hydrolysis rates of (A) amorphous PET film and (B) of crystalline PET powder by the WT enzyme at 30 °C (light blue), WT-40 °C (dark blue), DM enzyme incubated at 30 °C (light orange), and DM-40 °C (dark orange) were fitted using Equation S1, and fits are shown by dashed lines. (B) The WT enzyme at 40 °C on crystalline PET powder showed a decline in initial reaction rates at higher solids loadings. The dotted line (dark blue) indicates the fit of the data using Equation S1 until the drop (0–58 g L^{-1} PET) for the WT enzyme at 40 °C. Error bars represent the standard deviation of reactions performed in triplicate. Datasets are in Dataset S3.

Table 1. Kinetic parameters derived from conventional and inverse Michaelis-Menten plots at 30 and 40 °C for WT and DM. Error represents the standard deviation of fitting triplicate measurements.

	Conventional model parameters				Inverse model parameters			
	Amorphous PET film		Crystalline PET powder		Amorphous PET film		Crystalline PET powder	
	Conventional K_m [g L^{-1}]	k_{cat} ($^{Conv}V_{max}/E_o$) [s^{-1}]	Conventional K_m [g L^{-1}]	k_{cat} ($^{Conv}V_{max}/E_o$) [s^{-1}]	Inverse K_m [nM]	$k_{cat}\times\Gamma$[a] ($^{Inv}V_{max}/S_o$) [nmol s^{-1} g^{-1}]	Inverse K_m [nM]	$k_{cat}\times\Gamma$ ($^{Inv}V_{max}/S_o$) [nmol s^{-1} g^{-1}]
WT-30 °C	697 ± 179	1.5 ± 0.7	54 ± 1	0.8 ± 0.0	235 ± 18	0.2 ± 0.0	2162 ± 346	3.0 ± 0.7
WT-40 °C	87 ± 9	0.5 ± 0.0	26 ± 4	1.7 ± 0.2	309 ± 18	0.6 ± 0.0	2037 ± 314	5.8 ± 1.0
DM-30 °C	302 ± 5	0.5 ± 0.0	479 ± 86	0.5 ± 0.1	2690 ± 676	0.4 ± 0.2	1303 ± 13	0.2 ± 0.0
DM-40 °C	141 ± 6	0.5 ± 0.1	95 ± 11	1.2 ± 0.2	527 ± 26	0.5 ± 0.0	1874 ± 367	2.2 ± 0.6

[a] Γ = Reactive site density (nmol reactive sites per g of substrate) (Equation S5).

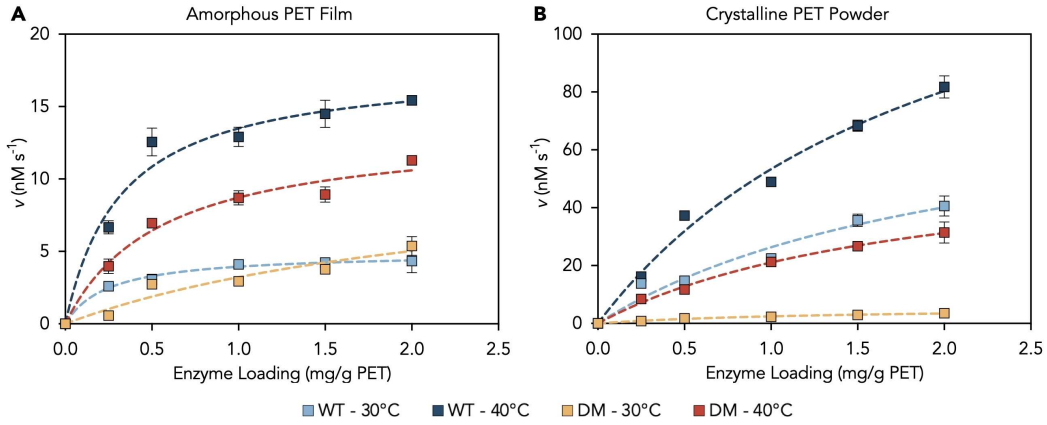

Figure 5. Inverse Michaelis-Menten plots at 30 and 40 °C. The plots show PET hydrolysis rates as a function of enzyme loading (mg enzyme per g PET). Square symbols represent turnover rates determined from experimental data using 2.9% substrate loading (29 g L^{-1}) and 0–2 mg g^{-1} enzyme loading (corresponding to 0–1.9 μM enzyme). The derived kinetic parameters can be found in Table 1. Hydrolysis rates of (A) amorphous PET film and (B) of crystalline PET powder by the WT-30 °C (light blue), WT-40 °C (dark blue), DM-30 °C (light orange), and DM-40 °C (dark orange) were fitted using Equation S2, and fits are shown by dashed lines. Error bars represent the standard deviation of reactions performed in triplicate. Datasets for these plots are provided in Dataset S3.

(corresponding to 0–1.9 μM enzyme) to identify a saturating enzyme load. The data are generally well-represented by the conventional (Equation S1) and inverse (Equation S2) MM equations (Figures 4 and 5). An exception to the conventional MM model is observed in the case of WT-40 °C on crystalline PET powder (Figure 4B). At 40 °C, the WT showed the expected behavior at low substrate loadings, but turnover rate decreases at higher substrate loadings (Figure 4B), leading to a poor fit of Equation S1 (Figure S6, Table S7). This behavior was not observed in previous interfacial kinetics studies using the same substrate;[15] however, in those studies only the DM was tested and the substrate loadings evaluated were much lower, encompassing 0–0.6% loading by mass (0–6 g L^{-1} PET). Data for the convMM plots using WT-40 °C on crystalline powder were fitted until the drop in turnover rate, from 0–58 g L^{-1} PET loading (Figure 4B).

The convMM and invMM datasets for each enzyme/temperature combination are in accord, showing that reaction velocities for the WT and DM are higher on the crystalline powder, except in the case of the DM at 30 °C. This increased reaction velocity is likely due to the higher surface area of the powder, and therefore increased availability of reaction sites. It is important to note that the powder is more crystalline (Table S2), and previous studies suggest that the amorphous regions of the polymer are preferentially depolymerized by PET hydrolases.[16] Regardless, the WT and DM generally show higher affinity (based on $^{conv}K_m$ values) and catalytic efficiency (based on the specificity constant = $^{conv}k_{cat}/^{conv}K_m$, Table S8) for the powder substrate compared to the amorphous film. Comparison of derived kinetic parameters from the convMM datasets (Table 1) reveals that while there is variation in catalytic rate (k_{cat}) across enzymes, temperatures, and substrates, the range is not overly large. This is unexpected, given the increase in reaction temperature.[17] Rather, there is a large variation in $^{conv}K_m$ across enzymes and temperatures. The $^{conv}K_m$ values drop significantly between the 30 and 40 °C reactions for both enzymes on both substrates, indicating there is a temperature dependence for affinity between the enzyme and the substrate. On amorphous film, the specificity constant of the WT incubated at 30 °C is comparable to the DM incubated at 30 °C, and similarly WT-40 °C is comparable to the DM-40 °C (Table S8). On crystalline PET powder, however, the WT has much higher specificity than the DM at both temperatures (Table S8).

Comparison of the derived kinetic parameters from the invMM datasets (Table 1) shows that WT requires less enzyme to reach saturation on amorphous PET. As one might expect, on

powder, the concentration of enzyme needed to saturate the substrate is significantly higher, with $^{inv}K_m$ values between 3 and 10 fold higher than on film. The 40 °C datasets achieve the highest maximal reaction velocity per available reactive site ($^{inv}V_{max}/S_o$), which provides a measure of nmol (product released) $s^{-1}g^{-1}$ (substrate). For all datasets, save DM at 30 °C, this parameter is between 5 and 20 fold higher on powder compared to film. The reactive site density, Γ, provides the concentration of reactive sites available per g of substrate (calculated values for Γ are in Table S8). Notably, the reactive site density calculated for the WT on crystalline powder is higher than the DM on the same substrate.

Kinetic parameters derived from initial rates are not predictive of reaction productivity over longer reaction times

Substrate loading, extent of conversion, residence time, and enzyme loading are key performance metrics that drive process cost for enzymatic PET recycling.[9b] Evaluation of reaction productivity as a function of enzyme loading and substrate loading can thus help identify optimal process conditions. To that end, we measured product release over 96 h for the WT enzyme at 30 and 40 °C and for the DM enzyme at 40 °C, evaluating the impact of substrate loading and enzyme loading on performance over three productivity measures: the rate of aromatic product release over a designated reaction duration (24 h in Figure 6A, D, G, 10 and 48 h in Figures S7 and S8), the rate of product release per unit of enzyme (Figure 6B, E, H), and percent conversion of the initial substrate (Figure 6C, F, I). All reactions used crystalline powder, substrate loadings of 2.9–23.2% by mass (29–232 $g L^{-1}$), and enzyme loadings of 0.5–3 mg enzyme per g PET.

For optimization of total product release per unit of time, evaluation of the reactions at 24 h shows that increasing the substrate loading and the enzyme loading yields the highest concentrations of product release per hour (Figure 6A, D, G). Performance was also evaluated at 10 and 48 h to evaluate different reaction times (Figures S7–S9). For all three reaction durations analyzed (10–48 h), the DM at 40 °C showed the highest overall product release rate (Figure 6G, Figures S7 and S8).

For optimization of product release rate per unit of enzyme in the reaction, after 24 h reaction time, two trends are observed. Reactions at 40 °C are optimized at high enzyme loadings and low substrate loadings (Figure 6E, H). In contrast,

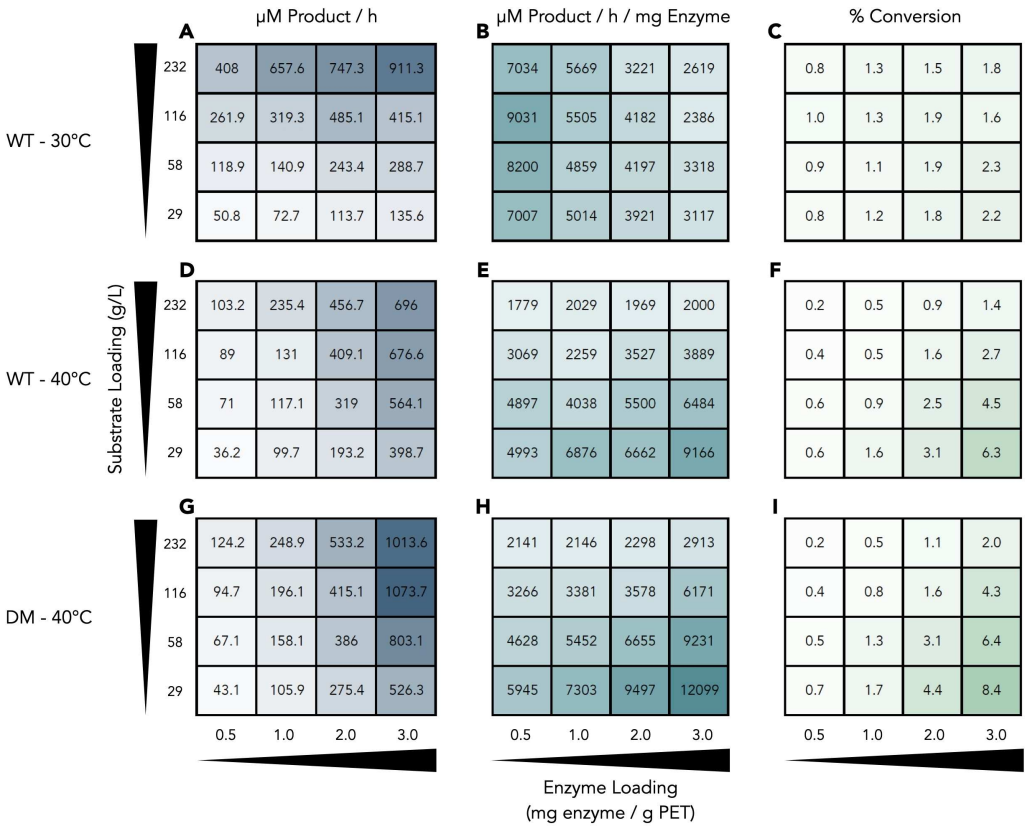

Figure 6. Functional catalytic performance as a function of enzyme and substrate loading. Comparative performance evaluation at 24 h for the WT enzyme at 30 and 40 °C and the DM enzyme at 40 °C using crystalline PET powder substrate. Performance is reported across three metrics: product release rate [µM h^{-1}], product release per unit of enzyme [µM h^{-1} mg^{-1} enzyme], and percent conversion of the substrate. Various enzyme and substrate loadings were tested for performance optimization. For substrate loadings, from least to most: 2.9% (29 $g L^{-1}$), 5.8% (58 $g L^{-1}$), 11.6% (116 $g L^{-1}$), and 23.2% (232 $g L^{-1}$); for enzyme loadings, from least to most: 0.5, 1, 2, and 3 mg g^{-1}. Color gradients facilitate identification of the best performance across the enzymes and temperatures tested. Additional comparisons at 10 and 48 h are presented in Figures S7 and S8, respectively. Progress curves for each dataset over 96 h are presented in Figure S9. Values used to derive this figure along with error, representing the standard deviation of triplicate measurements, are included in Dataset S4.

the WT incubated at 30 °C shows its highest hydrolytic rates at the lowest enzyme loading evaluated (0.5 mg enzyme per g PET) (Figure 6B). The DM enzyme incubated at 40 °C demonstrates the highest product release rates per mg of enzyme measured in this comparison at high enzyme loadings (2–3 mg enzyme per g PET) and the lowest substrate loading (29 g L^{-1}) (Figure 6H).

For optimization of the reaction based on substrate conversion, unsurprisingly, low solids loading and high enzyme loading result in the highest percent of depolymerization of the substrate for all reaction conditions tested (Figure 6C, F, I). Again, the DM at 40 °C demonstrates the highest overall conversion of the 29 g L^{-1} substrate samples (Figure 6I).

Increased PET conversion correlates with increased PET film crystallinity until a crystallinity threshold

Enzyme specificity as it relates to substrate crystallinity is a key economic and sustainability driver for biological PET hydrolysis.[9b] Improved rates (Table 1) and conversion extents (Figure 2) were observed for crystalline PET powder compared to amorphous PET film. To decouple the influence of increased solvent accessible surface area from the influence of substrate crystallinity in these observations, we examined product release using PET films with the same surface area and varying crystallinity. Conversion extent after 96 h was measured using an amorphous film (2.0 ± 1.6 % crystallinity), a biaxially oriented film (30.7 ± 5.5 % crystallinity), and annealed films with crystallinities ranging from 3.0 ± 1.7 to 25.1 ± 1.8 % (Figure 7, Figure S10A, Table S9). In general, conversion extent after 96 h increased as crystallinity increased until the percent crystallinity crossed a threshold around 20 % (Figure 7). Samples with 16.4 ± 1.2 % crystallinity show the highest product release, while a highly crystalline annealed film (25.1 ± 1.8 %) and the biaxially oriented film (30.7 ± 5.5 %) demonstrate low conversion extents (Figure 7).

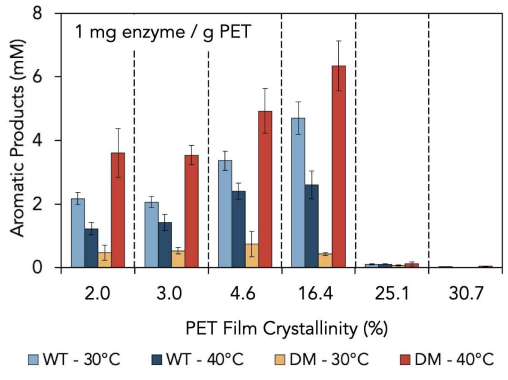

Figure 7. PET conversion as a function of substrate crystallinity. Total aromatic product release at 96 h for PET films with crystallinity ranging from 2.0–30.7 %. Films were approximately 0.25 mm thick. All reactions were performed with 2.9 % by mass (29 g L^{-1}) substrate loading and 1 mg g^{-1} enzyme loading at 30 or 40 °C. Error bars represent the standard deviation of reactions performed in triplicate. Data for reactions with 0.2 mg g^{-1} enzyme loading are in Figure S10B. The dataset for this figure is in Dataset S5. Data on annealed films used as substrates are in Figure S10A, Table S9.

WT and DM enzymes display different sensitivities to accumulation of depolymerization products

High extents of conversion will result in the accumulation of high concentrations of product monomer. To understand how monomer accumulation influences *Is*PETase, we first investigated the influence of monomer accumulation on BHET hydrolysis over a timescale that affords complete or near-complete substrate conversion. Using an initial substrate concentration of 2.25 mM BHET and 50 nM of the WT or DM, conversion was monitored over 18 h at 30 °C (Figure 8). For the WT, 12.0 ± 1.1 % of the initial substrate concentration remains after 18 h (Figure 8A), while for the DM only 1.4 ± 0.2 % remains (Figure 8D). To test the hypothesis that the WT is more susceptible to slowed hydrolysis due to accumulation of MHET, we next tested the same reaction scenario with both *Is*PETase and *Is*MHETase (50 nM each). With both enzymes present, the WT retains only 4.34 ± 0.4 % of the initial substrate (Figure 8B), while the DM in the presence of MHETase retains 27.9 ± 0.5 % of the initial substrate (Figure 8E), suggesting the DM is more susceptible to a slowed rate of hydrolysis with accumulated TPA.

To distinguish whether the effect of slowed hydrolysis was influenced by accumulating monomer or the presence of the second enzyme, we also evaluated how BHET hydrolysis was influenced by an initial concentration of monomer (1.25 mM MHET, TPA, or EG) in addition to the initial substrate concentration of 2.25 mM BHET. Over 18 h for the WT, BHET hydrolysis is slowed in the presence of excess MHET and EG, relative to the reaction containing only BHET. BHET hydrolysis is slightly improved in the presence of excess TPA (Figure 8C). For the DM, however, all three product monomers (MHET, TPA, and EG) slow the rate of BHET hydrolysis over 18 h (Figure 8F).

We subsequently investigated if accumulation of product monomers exhibits a similar effect on conversion of amorphous PET film over 96 h, again by initiating reactions in the presence of product (1.25 mM BHET, MHET, TPA, or EG) along with the PET film (2.9 % by mass or 29 g L^{-1}). Reactions containing 1 mg g^{-1} enzyme loading were evaluated for product release, accounting for the initial concentration of product monomer (Figure 9). For the WT incubated at 30 °C, product release is increased in the presence of TPA, and slowed by the accumulation of MHET and EG over time, relative to reactions containing only PET film (Figure 9A). For the DM, simulated accumulation of MHET had little effect on product release at 30 or 40 °C (Figure 9B, C). Simulated accumulation of TPA and EG show reduced product release at 30 and 40 °C (Figure 9B, C). To ensure the enzyme is not destabilized in the presence of EG or TPA, we also measured the thermal stability of both the WT and DM under increasing concentrations of each product. The apparent T_m did not change significantly in the presence of either monomer for concentrations ranging from 0–4 mM (Figure S12), indicating no denaturation or destabilization of the

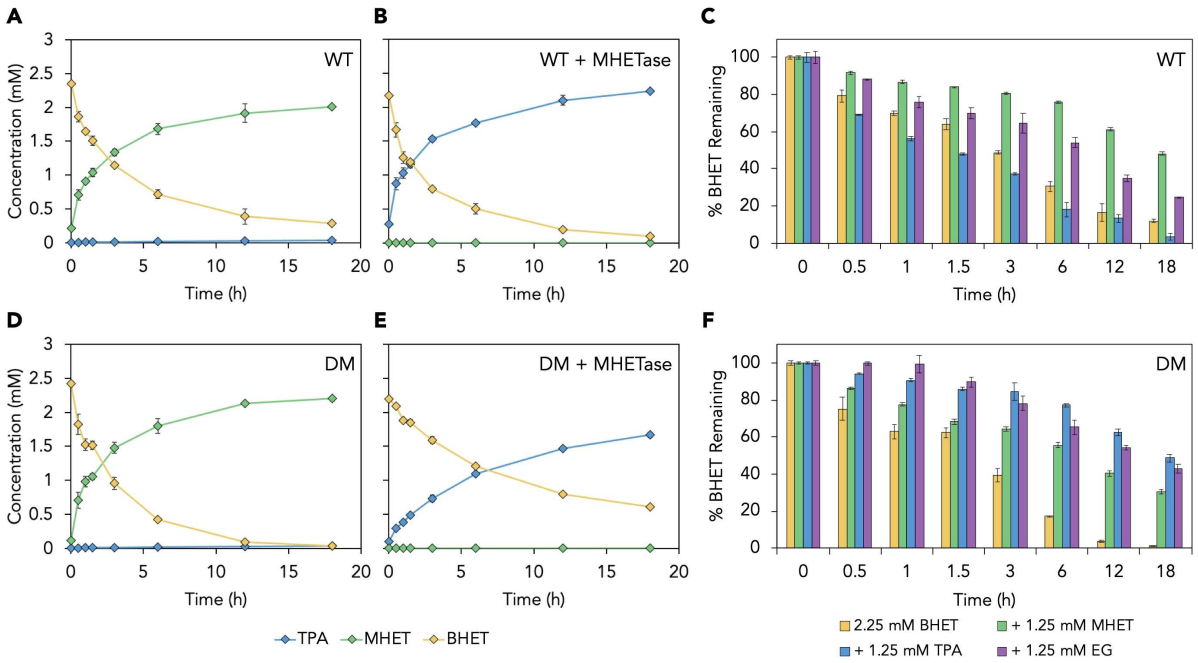

Figure 8. Accumulation of monomers influences extent of BHET hydrolysis at 30 °C. BHET hydrolysis was evaluated at 30 °C over 18 h reaction time using 50 nM of WT or DM PETase, or 50 nM WT or DM PETase and 50 nM MHETase. All reactions used a starting concentration of 2.25 mM BHET in reaction buffer. (A) BHET hydrolysis by the WT yields primarily MHET. Conversion of the initial 2.25 mM BHET supplied in the reaction is incomplete over 18 h reaction time. (B) Combining PETase WT and MHETase in the reaction increases extent of BHET conversion over 18 h. (C) Product accumulation for each of the constituent monomers is simulated by addition of 1.25 mM starting concentration to the initial BHET substrate. Bar graph shows % of initial BHET concentration remaining over 18 h reaction. In the presence of excess MHET (green) and EG (purple), the WT shows slower hydrolysis of BHET compared to the reactions containing BHET only. In the presence of excess TPA (blue), BHET hydrolysis is faster than reactions containing BHET only. (D) BHET hydrolysis by the DM yields primarily MHET. Conversion of the initial 2.25 mM BHET is nearly complete by 18 h. (E) Combining DM and MHETase in the reaction mixture yields primarily TPA. Accumulation of TPA appears to slow the conversion of BHET over the 18 h reaction observed. (F) When product accumulation is simulated, addition of excess MHET (green), TPA (blue), and EG (purple) all slow BHET hydrolysis by the DM compared to reactions containing only BHET. Panels A, B, D, and E represent datasets with a sample size of $n = 6$. Experiments in panels C and F were performed in triplicate. Error bars show the standard deviation across independent samples. Progress curves showing analyte concentrations for all datasets represented in panels C and F are shown in Figure S11. Figure datasets provided in Datasets S6–S8.

enzymes occurs in the presence of these monomers; this does not eliminate the possibility that these monomers interact with the enzyme.

Discussion

Enzymatic hydrolysis of waste PET holds promise for addressing accumulation of this abundant polyester. Accordingly, the major focus of enzymatic PET hydrolysis studies to date has been identification and engineering of new enzymes to this end. To address real waste streams at scale using an enzymatic recycling technology, additional process factors will be critical. Techno-economic analysis and life cycle assessment of such a process indicates that substrate loading, extent of depolymerization, reaction residence time, enzyme loading, and enzyme cost are all within the top 10 process considerations impacting the cost.[9b] Tolerance to product inhibition, specificity for the array of possible substrate morphologies (including high crystallinity substrates), and stability over the reaction residence time are also important considerations for minimizing process cost, and represent important challenges and opportunities for additional prospecting, characterization, and engineering of PET-hydrolyzing enzymes.

In this study, we compare the WT and a DM variant of the PET-hydrolyzing enzyme from *I. sakaiensis* across multiple factors that drive process costs, highlighting the effects these reaction variables can have on performance. For example, while the WT enzyme demonstrates high specificity for PET films under ambient conditions, there are limitations in enzyme stability (Figure 3). Techno-economic analysis of a modeled enzymatic PET recycling process shows that varying temperature (40–80 °C) imparts no change to process costs. In contrast, reaction residence time and enzyme price, both of which would be influenced by an unstable enzyme, contribute substantially to minimum selling price of the product.[9b]

Not only will structural and biophysical properties of the biocatalyst determine catalytic performance, but structural and physical properties of the substrate are also critical variables to consider.[13b,16e] We observe a range of catalytic activity depending on the characteristics of the substrate, as demonstrated using the annealed PET films of varying crystallinity (Figure 7, Figure S10). Both the WT and DM demonstrate a clear preference for more crystalline substrates, a trait that has not been reported for other PET-active enzymes. In the case of

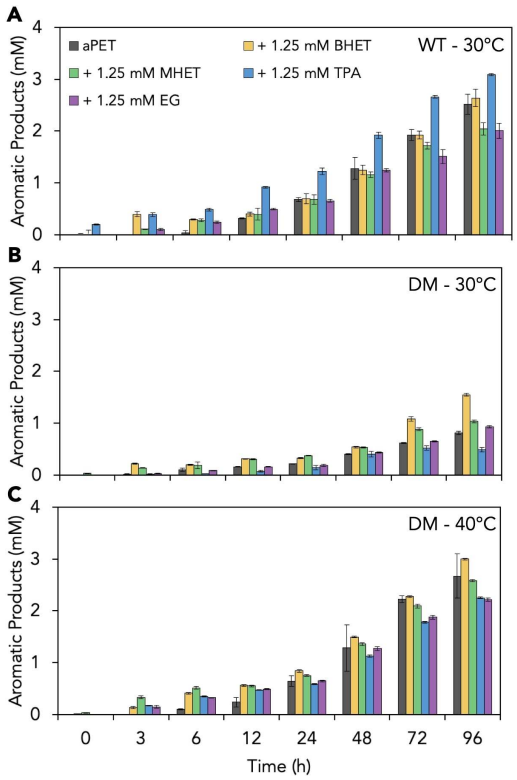

Figure 9. Accumulation of product monomers influences hydrolysis rates of amorphous PET film. Product accumulation was simulated through the addition of 1.25 mM monomer to the reaction mixture along with amorphous PET film substrate. Aromatic product accumulation over 96 h is compared to reactions containing only the amorphous PET film (gray). Monomer accumulation simulation was performed at (A) 30 °C with the WT, (B) 30 °C with the DM, and (C) 40 °C with the DM using 1 mg g^{-1} enzyme loading and 2.9% by mass (29 g L^{-1}) loading of the film for all reactions. Reaction progress is represented by the sum of aromatic products, BHET, MHET, and TPA, accounting for the starting concentration of product monomer. Error bars indicate the standard deviation of reactions performed in triplicate. Progress curves showing analyte concentrations are shown in Figure S13. Datasets provided in Dataset S9.

crystalline powder, the substrate also presents a high surface area, so continued work to deconvolute the influence of surface area and crystallinity on reaction rate and substrate affinity is worthwhile. In particular, it would be interesting to identify if PETase has a higher specificity for crystalline PET compared to other PET hydrolases, because while some enzymes have demonstrated remarkable hydrolytic activity on amorphized PET,[1e] far better than any activities reported for PETase or its variants, efficient degradation of highly crystalline substrates remains a key opportunity in the development of robust and cost-effective enzymatic depolymerization systems.[9b]

To further explain the differences observed between the WT and DM, it seems unlikely that the increased thermal stability of the DM is the primary driver of improved performance, as the DM enzyme at 30 °C shows the poorest performance, despite improved stability. It seems equally unlikely that a possible increase in PET polymer flexibility at 40 °C is the primary driver of improved performance, as the WT at 30 °C demonstrates nearly as good performance as the DM at 40 °C, still well below the PET T_g. The steady-state kinetic parameters derived from the convMM and invMM models suggest there is an important temperature-dependent change in affinity between the enzyme and the substrate at 40 °C, perhaps indicating that association between the enzyme and the substrate is better at 40 °C, but this is true for both enzymes. A temperature-dependent improvement in association between the polyester chain and the enzyme could explain this phenomenon, but whether that is due to increased flexibility of the polyester, or a conformational change of the enzyme is yet unknown.

Study of enzymes with specificity to PET has led to important discoveries about the catalytic mechanisms[4] and structural properties of the enzymes. Extending these discoveries to facilitate comparative biochemistry requires a balance of functional assessment and elucidation of meaningful kinetic parameters.[14] Functional assessment is critical for process development, uncovering relationships between time-dependence, dose-dependence, and conversion extent. Structure-function relationships, however, are traditionally studied through the comparison of kinetic parameters based on initial reaction rates. For either methodology of comparison, without consistent reaction conditions, direct comparisons between studies are challenging. In this study, we consider both approaches for comparing the WT and DM.

The typical model employed for derivation of kinetic parameters is based on the conventional MM theory. For interfacial biocatalysts, however, the applicability of this conventional model to reactions taking place at the interface of a solid substrate and aqueous media remains controversial,[14] specifically regarding the assumption that substrate be available in great excess relative to the enzyme concentration. To address the limited applicability of the conventional MM model for interfacial reactions, an alternative model has been proposed that instead looks at reaction regimes with a large excess of available enzyme, coined an "inverse" MM model.[14,15] This model has previously been applied to PET-hydrolyzing enzymes.[15]

In contrast to our observations, the previous interfacial kinetics study of the PETase DM showed that initial reaction rates declined in response to increased enzyme loading in the invMM reaction regime.[15] A hypothesis was proposed to suggest that "overcrowding" of active and/or denatured enzyme at the surface of the substrate, in combination with a reduction in the number of available reactive sites due to fast turnover of the substrate would lead to this inhibition behavior.[15] If limitation in surface accessibility were the primary cause, this inhibition behavior would be expected to occur more markedly on substrates with less surface area accessible, such as films, but that behavior is not apparent in the studies presented here.

With regard to satisfying the requirements of the conventional MM model, we selected an enzyme loading consistent with other experiments from this study, which also corresponds to the midpoint of the enzyme loadings using for the invMM experiment. This enzyme loading may have been too high to satisfy the requirements of the convMM model. From a "concentration" perspective, PET monomers comprising the

initial substrate load are in great excess of the enzyme, however we do not know the relative concentration of available reaction sites for these solid substrates a priori. The implications of this are that if the enzyme concentration is too high for the convMM dataset, at all solids loadings we observe here, the substrate is saturated with enzyme, and the requirement that substrate be in great excess is not met. For reference, the previous study[15] to look at initial reaction rates for PET hydrolysis used 30 nM enzyme loading (relative to 950 nM used in this study), but solids loadings up to only 0.6% (relative to 11.6% in this study). While this study uses approximately 30 times the enzyme concentration of the previous study, it also explores solids loadings of approximately 20 times higher as well. Despite the differences in experimental design, we observe a similar k_{cat} from the conventional model (0.52 s^{-1} reported by Bååth et al.[15] compared to 1.2 s^{-1} reported here) and a similar $^{inv}V_{max}/S_0$ from the inverse model (2.6 nmol s^{-1} g^{-1} from Bååth et al.[15] compared to 2.2 nmol s^{-1} g^{-1} reported here) when using the same enzyme, same substrate, and same temperature.

The kinetic parameters derived from these studies should allow one to compare performance of various enzymes, especially with regard to establishing structure-function relationships. The potential for performance based on the first moments or hours of a reaction, however, is not always reflective of functional performance. Based on the kinetic parameters derived from these studies, we would conclude that WT-40 °C is the superior enzyme/temperature combination, however the WT is less stable at 40 °C and the lifetime of this performance is limited relative to using the same enzyme at a lower temperature. Similarly, employing the DM at 40 °C, where it can maintain stability for longer, also allows for more PET conversion using the same amount of enzyme.

For any enzymatic process, but certainly for enzymatic reactions performed at an industrial scale, loss of catalytic performance due to inhibition can have a significant impact on process costs. Both the WT and DM enzymes show slowed rates of hydrolysis upon accumulation of product monomers. Each enzyme has a different inhibition sensitivity profile, which is somewhat unexpected. While we see potentially significant impacts of product inhibition at the small scale, we do not know if the influence is still significant at large scale. It is also an open question if the product accumulation profile and inhibition sensitivity profile might change in a pH-controlled reaction relative to the small-volume closed-system reactions we have presented here.[16b]

Conclusion

By evaluating the catalytic performance of the wild-type and double mutant *Is*PETase across several critical variables, we observe important and surprising differences between these closely related enzymes. This study highlights the importance of understanding and optimizing reaction variables that drive process cost from a holistic perspective, rather than focusing on individual characteristics of a biocatalyst.

Experimental Section

Descriptions of all materials and methods used in this study are detailed in the Supporting Information Appendix, Experimental Details.

Acknowledgements

This work was authored in part by Alliance for Sustainable Energy, LLC, the manager and operator of the National Renewable Energy Laboratory (NREL) for the U.S. Department of Energy (DOE) under Contract No. DE-AC36-08GO28308. Funding was provided by the U.S. DOE, Office of Energy Efficiency and Renewable Energy, Advanced Manufacturing Office (AMO) and Bioenergy Technologies Office (BETO). This work was performed as part of the Bio-Optimized Technologies to keep Thermoplastics out of Landfills and the Environment (BOTTLE) Consortium and was supported by AMO and BETO under contract no. DE-AC36-08GO28308 with NREL, operated by Alliance for Sustainable Energy, LLC. The BOTTLE Consortium includes members from the University of Portsmouth, funded under contract no. DE-AC36-08GO28308 with NREL and additionally supported by Research England (E3 Scheme). The views expressed in the article do not necessarily represent the views of the DOE or the U.S. Government. The U.S. Government retains and the publisher, by accepting the article for publication, acknowledges that the U.S. Government retains a nonexclusive, paid-up, irrevocable, worldwide license to publish or reproduce the published form of this work, or allow others to do so, for U.S. Government purposes. G.T.B., E.E., and N.A.R. also thank the NREL Laboratory Directed Research and Development program for funding. J.E.M. and A.R.P. thank Research England for E3 funding, and J.E.M. thanks the BBSRC for grant BB/P011918/1. T.S. and R.G. were funded through an NREL subcontract and University of Portsmouth Faculty of Science bursary. We thank the Diamond Light Source for beamtime (proposals MX-23269) and the beamline staff at I03 for support. We thank Ted Chapman and Ben Huckle at GSK, Worthing, for protein production and Mark Allen for initial structural work. We would also like to thank Richard K. Brizendine and Allison Z. Werner for helpful conversations in support of this work.

Conflict of Interest

The authors declare no conflict of interest.

Keywords: biocatalysis · chemical recycling · enzymes · PET hydrolase · polymers

[1] a) R. Wei, W. Zimmermann, *Microb. Biotechnol.* **2017**, *10*, 1302–1307; b) R. Wei, W. Zimmermann, *Microb. Biotechnol.* **2017**, *10*, 1308–1322; c) I. Taniguchi, S. Yoshida, K. Hiraga, K. Miyamoto, Y. Kimura, K. Oda, *ACS Catal.* **2019**, *9*, 4089–4105; d) F. Kawai, T. Kawabata, M. Oda, *ACS Sustainable Chem. Eng.* **2020**, *8*, 8894–8908; e) V. Tournier, C. M. Topham, A. Gilles, B. David, C. Folgoas, E. Moya-Leclair, E. Kamionka, M. L. Desrousseaux, H. Texier, S. Gavalda, M. Cot, E. Guémard, M.

Dalibey, J. Nomme, G. Cioci, S. Barbe, M. Chateau, I. André, S. Duquesne, A. Marty, *Nature* **2020**, *580*, 216–219.
[2] a) E. Herrero Acero, D. Ribitsch, G. Steinkellner, K. Gruber, K. Greimel, I. Eiteljoerg, E. Trotscha, R. Wei, W. Zimmermann, M. Zinn, A. Cavaco-Paulo, G. Freddi, H. Schwab, G. Guebitz, *Macromolecules* **2011**, *44*, 4632–4640; b) S. Sulaiman, S. Yamato, E. Kanaya, J.-J. Kim, Y. Koga, K. Takano, S. Kanaya, *Appl. Environ. Microbiol.* **2012**, *78*, 1556–1562; c) F. Kawai, T. Kawabata, M. Oda, *Appl. Microbiol. Biotechnol.* **2019**, *103*, 4253–4268.
[3] S. Yoshida, K. Hiraga, T. Takehana, I. Taniguchi, H. Yamaji, Y. Maeda, K. Toyohara, K. Miyamoto, Y. Kimura, K. Oda, *Science* **2016**, *351*, 1196–1199.
[4] B. C. Knott, E. Erickson, M. D. Allen, J. E. Gado, R. Graham, F. L. Kearns, I. Pardo, E. Topuzlu, J. J. Anderson, H. P. Austin, G. Dominick, C. W. Johnson, N. A. Rorrer, C. J. Szostkiewicz, V. Copié, C. M. Payne, H. L. Woodcock, B. S. Donohoe, G. T. Beckham, J. E. McGeehan, *Proc. Natl. Acad. Sci. USA* **2020**, *117*, 25476–25485.
[5] a) H. F. Son, I. J. Cho, S. Joo, H. Seo, H.-Y. Sagong, S. Y. Choi, S. Y. Lee, K.-J. Kim, *ACS Catal.* **2019**, *9*, 3519–3526; b) H. F. Son, S. Joo, H. Seo, H. Y. Sagong, S. H. Lee, H. Hong, K. J. Kim, *Enzyme Microb. Technol.* **2020**, *141*, 109656; c) Y. Cui, Y. Chen, X. Liu, S. Dong, Y. e. Tian, Y. Qiao, R. Mitra, J. Han, C. Li, X. Han, W. Liu, Q. Chen, W. Wei, X. Wang, W. Du, S. Tang, H. Xiang, H. Liu, Y. Liang, K. N. Houk, B. Wu, *ACS Catal.* **2021**, *11*, 1340–1350; d) E. Z. L. Zhong-Johnson, C. A. Voigt, A. J. Sinskey, *Sci. Rep.* **2021**, *11*, 928.
[6] H. P. Austin, M. D. Allen, B. S. Donohoe, N. A. Rorrer, F. L. Kearns, R. L. Silveira, B. C. Pollard, G. Dominick, R. Duman, K. El Omari, V. Mykhaylyk, A. Wagner, W. E. Michener, A. Amore, M. S. Skaf, M. F. Crowley, A. W. Thorne, C. W. Johnson, H. L. Woodcock, J. E. McGeehan, G. T. Beckham, *Proc. Natl. Acad. Sci. USA* **2018**, *115*, E4350–E4357.
[7] C. Roth, R. Wei, T. Oeser, J. Then, C. Föllner, W. Zimmermann, N. Sträter, *Appl. Microbiol. Biotechnol.* **2014**, *98*, 7815–7823.
[8] a) G. J. Palm, L. Reisky, D. Böttcher, H. Müller, E. A. P. Michels, M. C. Walczak, L. Berndt, M. S. Weiss, U. T. Bornscheuer, G. Weber, *Nat. Commun.* **2019**, *10*, 1717; b) H. Seo, S. Kim, H. F. Son, H.-Y. Sagong, S. Joo, K.-J. Kim, *Biochem. Biophys. Res. Commun.* **2019**, *508*, 250–255.
[9] a) L. D. Ellis, N. A. Rorrer, K. P. Sullivan, M. Otto, J. E. McGeehan, Y. Román-Leshkov, N. Wierckx, G. T. Beckham, *Nat. Catal.* **2021**, *4*, 539–556; b) A. Singh, N. A. Rorrer, S. R. Nicholson, E. Erickson, J. S. DesVeaux, A. F. T. Avelino, P. Lamers, A. Bhatt, Y. Zhang, G. Avery, L. Tao, A. R. Pickford, A. C. Carpenter, J. E. McGeehan, G. T. Beckham, *Joule* **2021**, *5*, 2479–2503.
[10] a) X. Han, W. Liu, J.-W. Huang, J. Ma, Y. Zheng, T.-P. Ko, L. Xu, Y.-S. Cheng, C.-C. Chen, R.-T. Guo, *Nat. Commun.* **2017**, *8*, 2106; b) C.-C. Chen, X. Han, T.-P. Ko, W. Liu, R.-T. Guo, *FEBS J.* **2018**, *285*, 3717–3723.
[11] T. Fecker, P. Galaz-Davison, F. Engelberger, Y. Narui, M. Sotomayor, L. P. Parra, C. A. Ramírez-Sarmiento, *Biophys. J.* **2018**, *114*, 1302–1312.
[12] M. Oda, Y. Yamagami, S. Inaba, T. Oida, M. Yamamoto, S. Kitajima, F. Kawai, *Appl. Microbiol. Biotechnol.* **2018**, *102*, 10067–10077.
[13] a) M. Barth, T. Oeser, R. Wei, J. Then, J. Schmidt, W. Zimmermann, *Biochem. Eng. J.* **2015**, *93*, 222–228; b) R. Wei, C. Song, D. Gräsing, T. Schneider, P. Bielytskyi, D. Böttcher, J. Matysik, U. T. Bornscheuer, W. Zimmermann, *Nat. Commun.* **2019**, *10*, 5581.
[14] J. Kari, M. Andersen, K. Borch, P. Westh, *ACS Catal.* **2017**, *7*, 4904–4914.
[15] J. A. Bååth, K. Borch, K. Jensen, J. Brask, P. Westh, *ChemBioChem* **2021**, *22*, 1627–1637.
[16] a) T. Brueckner, A. Eberl, S. Heumann, M. Rabe, G. M. Guebitz, *J. Polym. Sci. Part A* **2008**, *46*, 6435–6443; b) Å. M. Ronkvist, W. Xie, W. Lu, R. A. Gross, *Macromolecules* **2009**, *42*, 5128–5138; c) I. Donelli, G. Freddi, V. A. Nierstrasz, P. Taddei, *Polym. Degrad. Stab.* **2010**, *95*, 1542–1550; d) C. Gamerith, B. Zartl, A. Pellis, F. Guillamot, A. Marty, E. H. Acero, G. M. Guebitz, *Process Biochem.* **2017**, *59*, 58–64; e) R. Wei, D. Breite, C. Song, D. Gräsing, T. Ploss, P. Hille, R. Schwerdtfeger, J. Matysik, A. Schulze, W. Zimmermann, *Adv. Sci.* **2019**, *6*, 1900491.
[17] P. K. Robinson, *Essays Biochem.* **2015**, *59*, 1.

Manuscript received: September 9, 2021
Revised manuscript received: September 28, 2021
Accepted manuscript online: September 29, 2021
Version of record online: November 5, 2021